J. Chem Soc. Nigeria, Vol. 44, No. 1, pp 001 -010 [2019]

Synthesis, Characterization and Sorption Kinetics of Activated Alumina for Aqueous Phase Abatement of Toxic Metals.

A,U. Itodo, E.N. Iornumbe, O.M. Itodo and O.M. Fayomi
Department of Chemistry, Federal University of Agriculture, PMB 2373 Makurdi, Nigeria.

*Corresponding author: Email: itodoson2002@gmail.com, Tel: +2348039503463,

Received 09 October 2018; accepted 20 November 2018, published online 09 January 2019

ABSTRACT
The detoxification of simulated solution contaminated with lead and copper was achieved with activated alumina synthesized via direct method. The composite was characterized by various techniques, such as fourier transform infrared (FTIR) spectroscopy, scanning electron microscopy (SEM), Energy Dispersive X-ray spectrometer (EDX), EDS element mapping analysis and the metals concentration was estimated using the Atomic absorption spectroscopy (AAS). The synthesized activated alumina possessed nano-size morphology. The Sorption dynamics were investigated using various kinetics models and thermodynamic equations. Adsorption mechanism could be described with the pseudo-second order kinetics. Adsorption is spontaneous and endothermic.

Keywords: detoxification; divalent metals; Adsorbent; Adsorption, Diffusion

INTRODUCTION

Metal poisoning is the toxic effect of metals in certain forms and doses on life [1]. Toxic metals can be removed from human system through complexation, ion exchange, chelation and adsorption.
Adsorption is a process that occurs when an adsorbate accumulates on the surface on an adsorbent, forming a molecular or atomic film. Adsorption is operative in most natural physical, biological and chemical systems [2,3].

Adsorbents are usually used in granular form; it can vary in size from roughly 10 mm in diameter to as small as 50 nm. Important properties of adsorbents are adsorption capacity, density, specific surface area, porosity, selectivity and catalytic properties. Adsorbent porosity is the ratio of the volume of the pores and capillaries within the particle to the total volume of the particle [4].

Activated Alumina is an inorganic substance that is produced by the dehydration of aluminium hydroxide at high temperature. The material is highly porous and exhibits good surface area, resulting in superior adsorbent capabilities. It does not shrink, swell, soften or disintegrate when immersed in water and it is resistant to thermal shock and abrasion. Alumina possesses amphoteric properties allowing it to act as, either a base or an acid. The ability to alter its particle size or pores provides it with a spectrum of unique biological and physical properties that can address specific desiccant and /or separating needs. One of the important features of activated alumina is that it will bond with other substances without changing its chemistry or form [5].

Adsorption Kinetics

Most of the sorption desorption process of various solid phases are time dependent. Various kinetic models have been used by various researchers [6-8]

Pseudo first-order model: Lagergren pseudo-first order is widely used for the adsorption of an adsorbate from aqueous solution. The equation can be expressed as follows:

$$ln(Q_e - Q_t) = lnQ_e - k_t \quad (1)$$

Where Q_t is the amount of adsorbate adsorbed per unit of adsorbent (Mg/g) at contact time t (min), Q_e(Mg/g) is the amount of the adsorbate adsorbed per unit mass of the adsorbent, k_1 is the pseudo-first order rate constant (L/min). A linear plot of $ln(Q_e - Q_t)$ versus t gives the constant k_1 [6].

Pseudo- second- order model. The pseudo-second order kinetic as;

$$\frac{t}{q} = \frac{1}{K_2\ Q_e^2} + \frac{t}{Q_2} \quad (2)$$

Where K_2 is the pseudo- second order rate consent (g, mg^{-1} mm^{-1}). The initial adsorption rate, h(mg/gmin) and $h=k_2 Qe^{2\cdot}$ The slope from the linear plot of $\frac{t}{q}$ versus *t* gives the second rate constant, k_2 [7].

Elovich equation is generally expressed as;

$$\frac{dq_t}{dt} - \alpha \exp(-\beta q_t) \quad (3)$$

Where α is the initial adsorption rate ($mg \cdot g^{-1} \cdot min^{-1}$) β is the desorption constant ($g \cdot mg^{1}$) during any one experiment. A plot of *qt*vs ln(*t*) should yield a linear relationship with a slope of ($1/\beta$) and an intercept of ($1/\beta$) ln($\alpha\beta$) [8].

Adsorption Thermodynamic

According to Alessandro [9], adsorption of a chemical onto the surface of a solid adsorbent is achieved when the free energy of the adsorptive exchange is negative. Again, it has been observed that with increase in temperature, adsorption capacity decreases. The thermodynamic parameters such as the change in Gibb's free energy (ΔGº), change in entropy ΔSº and change in enthalpy ΔHº for the adsorption of dyes and metals have been determined using the equation:

$$\Delta G^0 = \Delta H^0 - T\Delta S^0 \quad (4)$$

The values of ΔHº and ΔSº are calculated from the slope and intercepts of the linear plot of ln k_{eq} versus 1/T.

Van't Hoff equation

In Van't Hoff model, *k* is equilibrium constant and R is the gas constant (8.314 J/mol).

From Eqn (4), $\Delta G^0 = \Delta H^0 - T\Delta S^0$

But $\Delta G^0 = -RT\ln(K_{eq})$ (5)

Therefore: $-RT\ln(K_{eq}) = \Delta H^0 - T\Delta S^0$ (6)

$$\ln(K)_{eq} = \frac{\Delta S^0}{R} - \frac{\Delta H^0}{RT} \quad (7)$$

$$\ln(K)_{eq} = \alpha \frac{1}{T} \quad (8)$$

The method is expressed graphically by the plot of $\ln(K_{eq})$ vs $\frac{1}{T}$

Where $\frac{\Delta H^0}{R}$ and $\frac{\Delta S^0}{R}$ is the slope and intercept respectively [10].

Arrhenius equation

This equation describes the temperature dependence on the rate of the reaction; the plot concerns the reaction rate constant in elementary reactions and can be mathematically stated as;

$$k = Aexp(Ea/RT) \quad (9)$$

$$ln\left(\frac{k_1}{k_2}\right) = \frac{Ea}{R}\left(\frac{1}{T_1} - \frac{1}{T_2}\right) \quad (10)$$

Where A is pre-exponential factor, Ea is the Arrhenius activation energy (-slope x R), *k* is the rate constant of reaction and R is the ideal gas constant. The plot is *ln* (*k*)vs 1/T. *ln* A is the intercept, while $\frac{Ea}{R}$ is the slope [3].

In this work, we synthesized, characterized and studied the adsorptive properties and dynamics of Activated Alumina for the removal of aqueous phase Lead and copper ions.

MATERIALS AND METHODS

Analytical grade reagents including aluminum chloride, sodium hydroxide, leads salt and copper salt were used. Routine lab equipment and glassware as well as instruments such as FT-IR spectrometer (Agilent technology), Scanning electron microscopy (SEM), Gas chromatography coupled with Mass Spectrometer detector (GC-MS; QP2010 Shimadzu, Japan), Energy Dispersive X-ray spectrometer (Carl Zeiss) were utilized in the characterization of adsorbents. Heavy metal quantification was achieved by Atomic Absorption Spectrometer (AAS).

Synthesis of activated alumina.

Activated Alumina was synthesized according to documented protocol [11]. Aluminium chloride (2.5g) was weighed into beaker. Distilled water (25 mL) was added and stirred with a glass rod until the solid dissolved. Solution was warmed to 40^0C and while stirring with a glass rod, 15 mL of 2 mol dm^{-3} sodium hydroxide solution was added, forming a white solid. The solid was allowed to settle and 1mL NaOH was added at a time, until the white precipitate changes colour to off white. This was followed by filtration.The white solid was washed from the beaker until it is completely transferred to the filter paper. When filtration was completed, distilled water was gently squirted over aluminium hydroxide on the filter paper to rinse it. Again, the liquid was allowed to filter away completely. Oven drying was carried out at 105^0C . The dried solid was scraped into the crucible and heated over a small non-luminous bunsen flame for 10 minutes. The crucible and contents was put in a desiccator to cool. The cooled crucible was weighed with the dried aluminum oxide in it. Al_2O_3 was activated by heating in an electric furnace at 500^oC for 24 h. The activation process was adopted to remove the physically adsorbed species present on the surface of alumina.

Characterization of prepared Adsorbent

The synthesized adsorbent was characterized using FT-IR for functional groups analysis; SEM analysis for surface morphology; EDX-ray was used to determine the elemental composition of the synthesized compound.

Batch Adsorption Experiments

For the adsorption experiments, documented protocol [12] was adopted with slight modification in sorbate/sorbent ratio.

Effect of Parametric factors

Parametric factors investigated include effect of concentration, pH; dosage and contact time [13]

Adsorption Kinetics and Thermodynamics

Data generated from sorption experiments was fitted into some Kinetic (pseudo-second –order model, Lagergren Pseudo first-order model and Elovich equation). and thermodynamic (Van't Hoff) equations

RESULTS AND DISCUSSION

The physicochemical characteristics of Activated Alumina (AA) are shown in Table 1.

Table 1: Physical properties of AA

Parameters	Result
Colour	White
Odour	Odourless
State	Solid
% Yield	85.2%
Melting point	$2{,}98^0$C

SEM Characterization

Figure 1a, b and c shows the SEM micrographs of synthesized activated alumina at 1500x magnification, SEM image of Activated Alumina loaded with Pb and SEM image of the spent adsorbent of AA loaded with Cu. The SEM images shows a clear surface available for the adsorption. This image also indicates the availability of pores and cracks on the surface of AA which may be one of the reasons for the significant increase in the adsorption capacity of the synthesized compound. Figures 1b and c demonstrate site occupancy. This could be as a result of the adsorbates (Pb and Cu) adsorbed onto the cavities of activated alumina. Similar results has been reported [14].

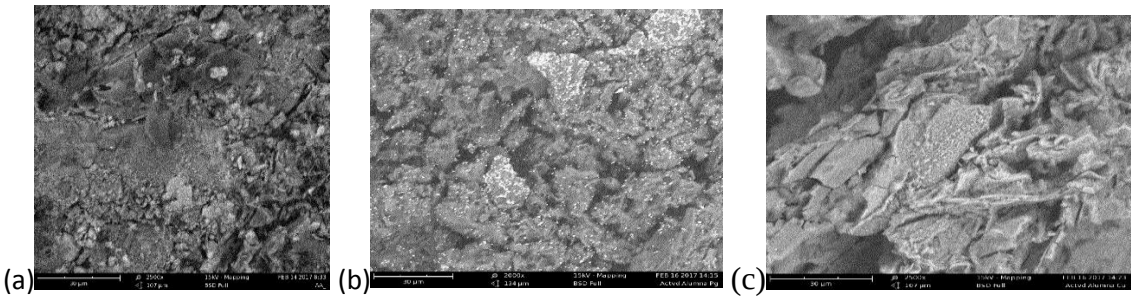

Fig. 1: SEM Images of (a) raw AA (b) Spent Pb-AA (c) Spent Cu-AA at 1500X Magnifications.

Energy Dispersive X-ray Spectroscopy (EDX).

Figure 2 is the EDX spectrum of AA majorly indicating O and Al and confirming Al_2O_3. The individual elements in the synthesized AA were represented by specific color in SEM's- Energy Dispersion Spectroscopy images (Figure 3a) and SEM's EDS element map (Figure 3b), obtained at low kV energy-dispersive spectroscopy (EDS), shows the distribution of elements, with Al and O having high composition in AA. This implied that oxygen is more abundant in the compound, Al_2O_3

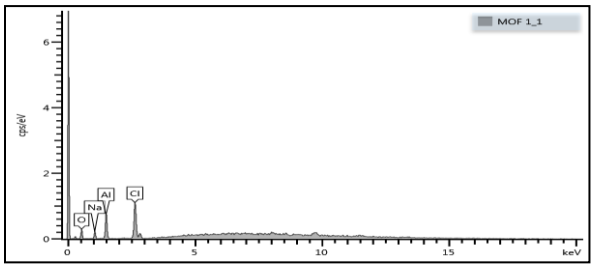

Figure 2: EDX Spectrum for activated alumina, indicating the presence of O, Na, Cl, and Al.

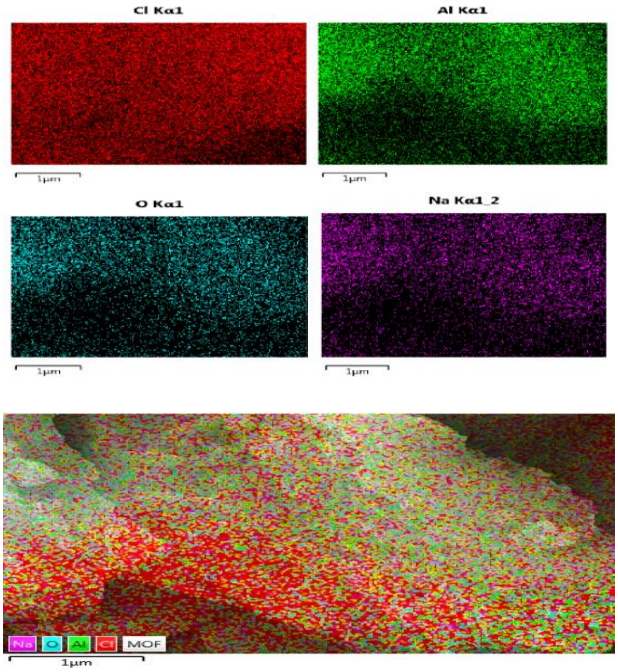

Quantitative Elemental Analysis using Ultra Plus Field Emission SEM

Table 2 shows the weight percentage compositions (w%) of the elements present in AA using FESEM quantification

Table 2: Elemental Composition of AA

AA	Wt.%
O	36.74
Na	7.96
Al	18.60
Cl	36.70
Total	100.00

FTIR Analysis of Adsorbents

The FTIR spectral for activated alumina is shown in Figure 4, while Table 3 shows FTIR characteristics of AA and spent AA. Both adsorbents possessed similar FTIR spectra, with little differences because of the loading of the adsorbates. A broad band extending around 511.01 for the virgin AA, is due to symmetric bending of O-Al-O [15].

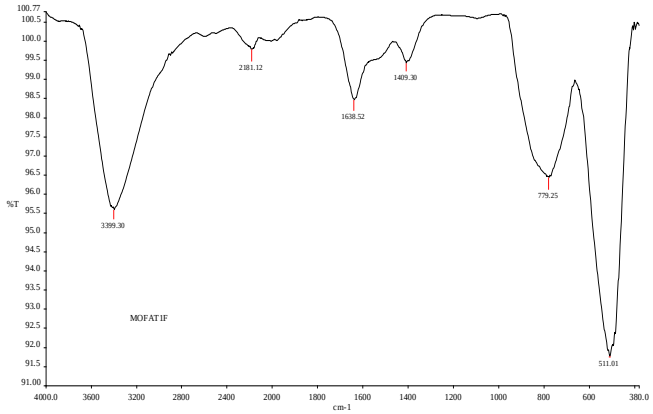

Figure 4: FTIR Spectrum for Activated Alumina.

Figure 3 SEM's (a) EDS Images of Elements (b) EDS

Map Showing Distribution of the Elements.

Table 3: FTIR Spectra Characteristics of AA and spent AA.

Vibrational Frequency (cm^{-1})	Characteristics Functional group	Raw AA	Observed Frequency (cm^{-1})		Assignment
			Spent AA-Pb	Spent AA-Cu	
3500-3200	O-H stretch H- bonded	3399.30	3496-3391	-	Alcohols, Phenols
3000-2500	O-H stretch	-	-	2885, 2776	Carboxylic Acids
2260-2100	-C-C- stretch	2181.12	2187	-	Alcohols, phenols
1680- 1640	-C=C- stretch	1638.52	1640	-	Alkenes
600- 400	M-O	511.01	-	-	Metal oxide

Batch Adsorption Studies

The effects of contact time, Adsorbent dosage, pH, temperature and initial metal concentrations were studied. Figure 5 shows the effects of parametric factors on Percentage removal of Pb and Cu on AA.

Effect of adsorbent dosage

The effects of varying adsorbent doses of AA were investigated for the removal of lead and copper from metal solution. The removal of Pb by AA was found to be highest when the adsorbent dosage was 0.09 g achieving a percentage removal of 95.9% (Figure 5). The increase in removal of Pb with adsorbent dose can be attributed to the introduction of more binding sites for adsorption. The removal of Cu by AA was found to be highest when the adsorbent dosage was 0.03 g achieving a percentage removal of 75.35%, after which there is a decrease in the percentage removal of the

adsorbate as the adsorbent dosage increases. This may be attributed to two reasons; (i) a large adsorbent amount effectively reduces the unsaturation of the adsorption sites and correspondingly, the number of such sites per unit mass comes down resulting in comparatively less adsorption at higher adsorbent amount .(ii) Higher adsorbent amount creates particle aggregation, resulting in a decrease in the total surface area and an increase in diffusional path length both of which contribute to decrease in amount adsorbed per unit mass. Similar results have been reported [16].

Effect of pH

From the result shown in Figure 5, It was seen that the lowest percentage removal was recorded when the pH was low for the Pb and Cu metal solution and at the peak when at pH 6, achieving the percentage removal of 95.9% and 96.2% removal of Pb and Cu respectively. When the pH becomes basic a decrease in the percentage removal was observed. These observations could be linked to higher concentration of H^+ ion in the solution which competes with the metal solutions in the pH of 2 and 4 [17].

Effect of contact time

From Figure 5, it was also observed that as the contact time increases, the percentage adsorption removal of the lead on AA also increases progressively until all the active adsorptive sites have been filled and an equilibrium is reached at 240 mins. In an experiment involving the adsorption of copper by AA, it was observed that, as the contact time increase, the percentage removal of the metal ion also increases. This may be as a result of the availability of binding sites [18].

Effect of temperature

From the experiment investigated on the adsorption of lead by AA, it was observed that adsorption capacity increases as the temperature increases while keeping other parameters constant (Figure 6). The improved adsorption capability with increasing temperature suggests that the adsorption is an endothermic one. This trend may be due to the tendency of Pb ions gaining more kinetic energy to diffuse from the bulk phase to the solid phase with an increase in solution temperature. it was observed that, as the temperature was increasing, the percentage removal of the Cu by AA was decreasing. This could be as a result of increase in temperature that leads to increase in kinetic energy of the metal ions and therefore weakening the forces of attraction between the metal ions and the adsorbent. It also suggests that the adsorption process is an exothermic one [19].

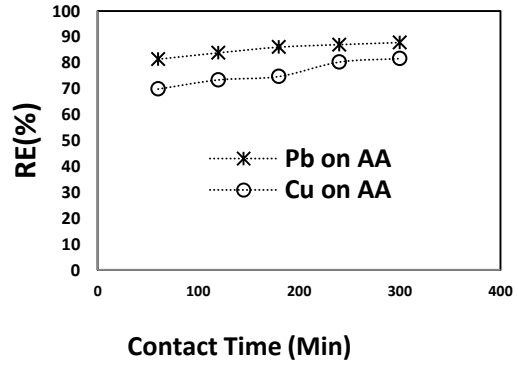

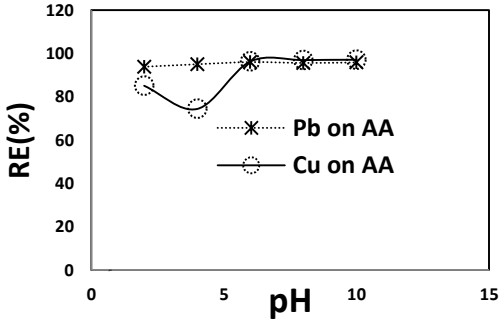

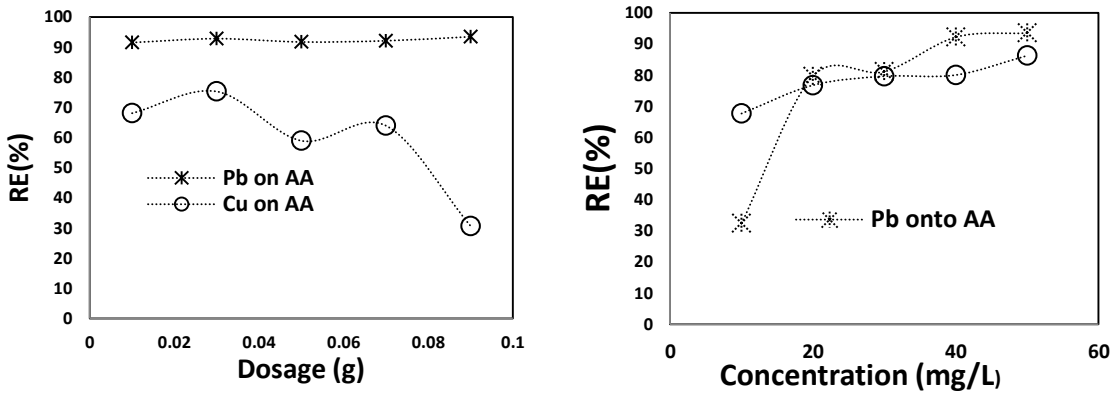

Figure 5: Effects of Parametric Factors on Percentage Removal of Pb and Cu on AA

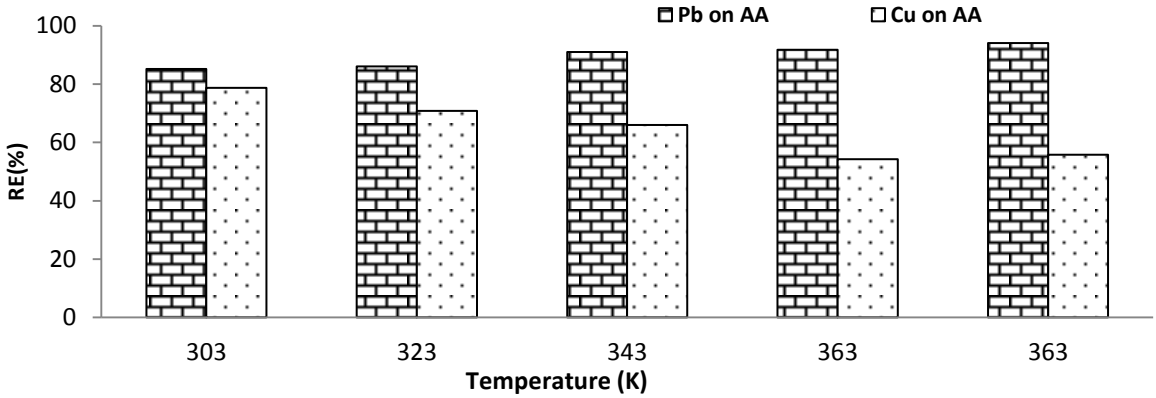

Figure 6. Effects of Temperature on the Percentage Removal of Pb and Cu onto AA.

Adsorption Kinetics.

The adsorption kinetic plot of Pb and Cu on AA is shown as Figure 7. Table 4 shows the kinetic studies experimental constants for Pb and Cu on AA. The study of adsorption dynamics describes the solute uptake rate and evidently this rate controls the residence time of adsorbate uptake at the solid-solution interface. Taha *et al*. [20] inferred that kinetic models help in the study of adsorption rate, model the process and predict information about adsorbent/adsorbate interaction

The rate constant of adsorption is determined from the first-order equation given by Langergren and Svenska [21]. The R^2 values for the First-order model are 0.988 and 0.804 for Pb and Cu onto AA respectively (Table 11). This model considers that the rate of adsorption sites occupation is proportional to the number of unoccupied sites.

The coefficient of regression for the pseudo-second order model are 0.999 and 0.976 for Pb and Cu onto AA respectively. This suggests the applicability of the pseudo-second order kinetic model to describe the adsorption process of Pb and Cu uptake on the activated alumina. This also shows that the overall rate of the adsorption process was controlled by chemisorption and involves valency forces through sharing or exchange of electrons between the sorbent and the sorbate [22]. The second-order kinetics is applicable to the system; since the plot of t/qt versus t, gave a linear relationship.

Elovich equation was adopted to model adsorption of Pb onto AA**.** R^2 for this model is 0.994 and 0.945 for Pb and Cu onto AA respectively. This

shows that the rate determining step of the adsorption process is diffusion in nature [23].

Thermodynamic Studies for AA.

The adsorption thermodynamic plots of the adsorption of Pb and Cu on AA are shown in Figure 8. Table 5 shows the thermodynamic parameters for Pb and Cu onto AA. The R^2values for Pb and Cu onto AA were 0.940 and 0.941. This shows good applicability of the Vant Hoff equation.

The calculated thermodynamic parameters were listed in Table 5. The negative values of ΔG^o at the temperature studied indicate the spontaneous nature of Pb and Cu adsorption by AA. The negative value of ΔH^o confirms the exothermic nature of adsorption process and also that the adsorption is physical in nature with weak forces of attraction and a decrease in randomness at sorbent/sorbate interface during the adsorption process while the positive value in ΔH^o as in the case of Cu onto AA indicates the reaction is endothermic [24].

Table 4: Kinetic studies experimental constants for Pb and Cu adsorption onto AA.

Kinetic Model	Constants	Values AA-Pb	Values AA-Cu
First Order	R^2	0.988	0.804
	k_1 (min^{-1})	-0.0051	-0.005
Pseudo-Second Order	R^2	0.999	0.997
	k_2 (g/g min)	7.0×10^{-5}	6.0×10^{-5}
Elovich	R^2	0.994	0.911
	α (mg g^{-1} min^{-1})	1.468	0.817
	β (mg g^{-1})	6.353	3333.33

Table 5. Thermodynamic Parameters for Pb and Cu onto AA

Parameters	Values AA-Pb	Values AA-Cu
R^2	0.9406	0.941
ΔS (KJ/mol)	45.860	-44.712
ΔH (KJ/mol)	12488.5	-13963.3
ΔG(Kj/mol.K)	-31322	-1843.01

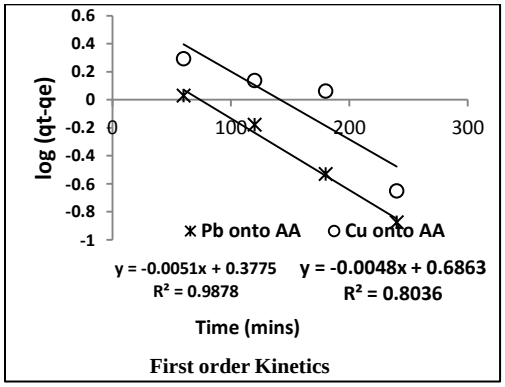

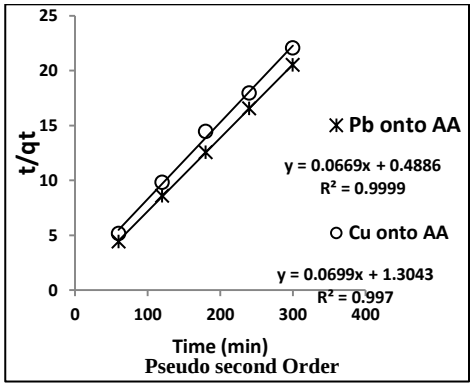

Figure 7: Adsorption Kinetic Plots of Pb and Cu on AA.

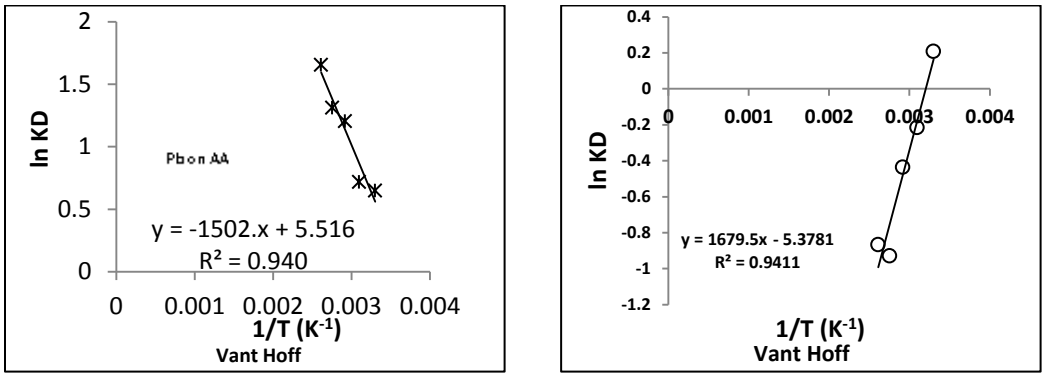

Figure 8: Vant Hoff Plots of Pb and Cu onto AA.

CONCLUSION

Activated alumina was successfully synthesized via a simple direct method and widely characterized. Adsorbent's affinity for metal ions in simulated waste water was investigated via batch sorption techniques. Kinetic studies indicated that all the choice models gave high positive correlation with the pseudo second-order model giving a better linearity. These results suggested that the derived Activated alumina can find application as a low-cost adsorbent for copper and lead ion detoxification to > 90 % removal efficiency. Deductions from thermodynamic parameters revealed a spontaneous ($-\Delta G^o$), exothermic ($-\Delta H^o$) and physical adsorption processes for Pb uptake. Overall highlights from this work support a generalization that alumina type of absorbent could possibly become one of the most beneficial absorbent for environmental remediation.

REFERENCES

1. I. Egbuna, A. Bose (2004). Acute Aluminum Neurotoxicity Secondary to Treatment of Severe Hyperphosphatemia of Acute Renal Failure and the K/DOQI Guidelines: A Case Report and Review of the Literature. ,*Internet Journal of Nephrology.* **34** : 456-651.

2. R. Gottipati, S. Mishra (2012). Application of Response Surface Methodology for Optimization of Cr(III) and Cr(VI) adsorption on Commercial Activated Carbons. *Research Journal of Chemical Sciences.* **2**: 40-48.

3. S. Khattri, M. Jekel, M. Singh (2009). Removal of Malachite Green from Dye Wastewater using Neem Sawdust by Adsorption. *Journal of Hazardous Material.* **I67**:1089-1094.

4. A. Buekens, N. Zyaykina (2001). Adsorbents and Adsorption Process for Pollution Control, Pollution Control Technologies. Vol.II. Encyclopedia of Life Support Systems.

5. H. Tahi, M. Saleem, M. Afzal, H. Ahmad, S.T. Hussain (1998). Removal of Chromium from Tannery Waste using Zeolite–3A. *Adsorption Science Technology.* **16**: 153–161.

6. T. Ru-Ling, W. Feng, J. Ruey-Shin (2013). Characteristics and Applications of the First Order Equation for Adsorption Kinetics. *S.Korea Journal on Science.* **5**: 231-433.

7. I.O. Oboh, E.O. Aluyor , T.O. Audu (2013). Second –order Kinetic Model for the Adsorption of Divalent Metal Ions on Sidaacuta leaves. *Corporative Research Center*. **43**: 222-321.

8. W. Badmus (2007). Second - Order Kinetic Model for the Sorption of Cadmium onto Free fern: A Comparison of Non- Linear Method. *Proceedings of the Chemical Society*. P.90-108

9. D.S. Alessandro (2000). Factors Affecting Sorption of Organic Compounds in Natural

Sorbent Water Systems: A Review, Environmental Department, AMB-TEIN, Via Anguillarese 301, 00060 Rome, Italy.

10. G. Darawsk (2001). The Adsorption Kinetics of the Cationic Dye Methylene Blue onto Clay. *Journal Hazardous Materials*. **11**: 217-228.

11. P. Hajira, Q. Fahin (2001). Defluoridation of Water with Activated Alumina : batch operations. *Indian journal of Envi. Health.* **30** : 262-299.

12. Y. Song, S. Ding, S. Chen, X. Hui, M. Ye, R. Jianmin (2015). Removal of malachite green in aqueous solution by adsorption on sawdust. ,*Korean J. Chem. Eng.***32**: 2443–2448

13. H.Y. Naeema (2014). Removal of Toxic Copper Ions using Alumina. ,*Int. Journal of Current Microbiology and Applied Science*. **4** : 415-431.

14. J.B. Rompicherla, M. Utkarsh, G. Suresh (2015). Synthesis and Use of Alumina NPs as an Adsorbent for the Removal of Zn(II) and CBG from Wastewater. *Macedonian J. Chemistry and Chem. Eng***.. 6**: 31–41.

15. H.S. Lee, N. Kim, T.J. Park, M.K. Lee (2015). Synthesis and Characterization of Metallic Oxides, *Chem. Eng. J.*. **230**: 351–360.

16. M.P. Pons, C.M. Fuste (1993). Uranium Uptake by Immobilized Cells of Pseudomonas Strain EPS 5028, *Applied Microbiology Biotechnology* **39**: 661-665.

17. W. Rudzinski, W. Plazinski (2009). On the applicability of the pseudo-second order equation to represent the kinetics of adsorption at solid/solution interfaces. *Adsorption*. **15**: 181

18. N. Boldizsar, M. Carmen, M. Andrada. I. Cerasella, L. Barbu-Tudoran, M. Cornelia (2014). Linear and Non-linear Regression Analysis for Heavy Metals removal using Agaricusbisporus Macro Fungus. *Arabian Journal of Chemistry*. 32: 554-653

19. O.A. Oyedeji, G.B. Osinfade (2010). Removal of Copper (II), iron (III) and Lead (II) Ions from Mono-component Simulated Waste Effluent byAdsorption on Coconut Husk. *African Journal of Env. Sci. and Tech*. 4: 382-387

20. M.E. Taha, H.M. Zeinhom, S. Walied, M.I. Ahmed (2014). Kinetic and Isotherms Studies of Adsorption of Pb (II) from Water onto Natural Adsorbent. *J. Env. Protection.* **5**: 1667-1681.

21. B. Olugbenga, M. Oladipo, A. Misbaudeen, A. Olalekan (2010). Kinetic and Equilibrium Studies of MB Removal from Aqueous Solution by Adsorption on Treated Sawdust. *Macedonian J. Chem. and Chem. Eng.*. **29**: 77–85.

22. Y.S. Ho, G. McKay (1999). Pseudo-Second Order Model for Sorption Processes. *Biochemistry* **34**: 735-742.

23. S. Chakrapani, V. Babu, R. Somasekhara (2009). Adsorption Kinetics for the Removal of Fluoride from Aqueous Solution by Activated Carbon Derived from the Peels of Selected Citrus Fruits. *E- Journal of Chem.* **7**(S1): S419-S427

24. N. Atar, A. Olgun, B.S. Wang (2012). Adsorption of Cadmium (II) and Zinc (II) on Boron Enrichment Process using Polyaniline Nanocomposite Coated on Rice Husk. *Iranica Journal of Energy* **67**: 655-794.